

# Correlated-basis description of $\alpha$ -cluster and delocalized $0^+$ states in $^{16}\text{O}$

W. Horiuchi<sup>1</sup> and Y. Suzuki<sup>2,3</sup>

<sup>1</sup>*Department of Physics, Hokkaido University, Sapporo 060-0810, Japan*

<sup>2</sup>*Department of Physics, Niigata University, Niigata 950-2181, Japan*

<sup>3</sup>*RIKEN Nishina Center, Wako 351-0198, Japan*

A five-body calculation of  $^{12}\text{C}+n+n+p+p$  is performed to take a step towards solving an outstanding problem in nuclear theory: The simultaneous and accurate description of the ground and first excited  $0^+$  states of  $^{16}\text{O}$ . The interactions between the constituent particles are chosen consistently with the energies of bound subsystems, especially  $^{12}\text{C}+n$ ,  $^{12}\text{C}+p$ , and  $\alpha$ -particle. The five-body dynamics is solved with the stochastic variational method on correlated Gaussian basis functions. No restriction is imposed on the four-nucleon configurations except the Pauli principle excluding the occupied orbits in  $^{12}\text{C}$ . The energies of both the ground and first excited states of  $^{16}\text{O}$  are obtained in excellent agreement with experiment. Analysis of the wave functions indicates spatially localized  $\alpha$ -particle-like cluster structure for the excited state and shell-model-like delocalized structure for the ground state.

PACS numbers: 21.60.-n, 21.10.-k, 27.20.+n, 21.60.Gx

The nucleus  $^{16}\text{O}$  is doubly magic and tightly bound. Its  $0^+$  ground state is regarded to have predominantly spherical closed shell structure. Contradicting the nuclear shell-model filling of single-particle orbits, however, the first excited state of  $^{16}\text{O}$  has positive parity,  $J^\pi = 0^+$ , with the unexpectedly low excitation energy  $E_x=6.05\text{ MeV}$ . Its appearance was therefore mysterious. A conventional idea is to explain the excited  $0_2^+$  state with multi-particle multi-hole, especially 4p-4h, excitations. The physics mechanism behind such excitations is believed to originate from nuclear deformation [1], and the appearance of spherical and deformed states observed in several nuclei is called shape coexistence [2, 3]. The essence of the phenomenon lies in that two states with identical quantum numbers are realized at close energies. Understanding the coexistence mechanism can thus be a general, interesting problem for other quantum many-body systems as well.

Recent theoretical works have focused on the first excited state of  $^{16}\text{O}$  with various approaches. Based on the harmonic-oscillator (HO) shell-model the possibility of selecting important basis states with symplectic algebra [2] or the modification of single-particle energies [4] has been discussed. Beyond mean-field approaches have been tested in configuration mixing calculation of Slater determinants [5, 6]. Though the energy gain of the 4p-4h state is found to be substantial in the generator coordinate method, its component in the  $0_2^+$  state is not very large [5]. The basis states in Ref. [6] are generated by an imaginary-time evolution of stochastically selected single-particle Gauss packets, allowing for  $^{12}\text{C}+\alpha$ -like configurations, but the excitation energy of the  $0_2^+$  state is too high. Large-scale *ab initio* calculations with the no-core shell model [7] and the coupled-cluster theory [8] have been performed but the energy of the  $0_2^+$  state is still so high in the current model space that more computational efforts appear to be required to reproduce its excitation energy.

It was reported about 40 years ago [9] that all  $T = 0$

levels of  $^{16}\text{O}$  but the  $10.96 (0^-)$  state below  $E_x = 15\text{ MeV}$  are reproduced by a semi-microscopic  $^{12}\text{C}+\alpha$  two-cluster model where the excitation of  $^{12}\text{C}$  and the Pauli principle are taken into account. A microscopic version of the similar cluster model also succeeded in reproducing the two  $0^+$  states [10]. The success seems to suggest that the structure of the  $0_2^+$  state is closely related to the tight binding of  $\alpha$ -particle, that is, the four particles tend to form an  $\alpha$ -cluster [11]. It should be noted that the cluster model space includes some deformation and for low HO excitations has significant overlap with symplectic basis states [12].

In this paper we report a first converged five-body calculation of a  $^{12}\text{C}$  core plus four (valence) nucleons ( $4N$ ) for the  $0^+$  states of  $^{16}\text{O}$ . This is an extension of the work [9] towards a more microscopic direction in that no preformed  $\alpha$ -cluster is assumed. The excitation of  $^{12}\text{C}$  is ignored. Regarding the core as  $0p_{3/2}$  closed configuration, we impose the Pauli requirement that the valence nucleon be free from the occupied orbits. Except for that the model has no restriction on the valence nucleon orbits, and hence can accommodate not only 0p-0h, 2p-2h, 4p-4h, etc. but also  $^{12}\text{C}+\alpha$  configurations. To be realistic, both the core-nucleon ( $CN$ ) and the two-nucleon ( $NN$ ) interactions are chosen consistently with the energies of relevant subsystems, especially  $^{13}\text{C}$  ( $^{13}\text{N}$ ) and  $\alpha$ -particle. We also treat  $^{16}\text{C}$  as the  $^{12}\text{C}$  core plus four neutrons to examine how the  $nn$  and  $np$  interactions affect the structure.

The five-body system we consider here is described with the following Hamiltonian

$$H = T_v + T_{cv} + V_v + V_{cv}. \quad (1)$$

The total kinetic energy consists of the kinetic energy of the  $4N$  ( $T_v = \sum_{i=1}^4 T_i - T_{c.m.}$ ) relative to their center of mass (c.m.) and the kinetic energy for the relative motion ( $T_{cv}$ ) between the  $4N$  c.m. and the core. The total potential energy also consists of two terms,  $V_v = \sum_{i<j} v_{ij}$  and  $V_{cv} = \sum_{i=1}^4 U_i$ . The term  $v_{ij}$  rep-

resents the  $NN$  potentials between  $i$ th and  $j$ th valence nucleons, and  $U_i$  is the  $CN$  potential acting on the  $i$ th nucleon. The former is taken from the central Minnesota (MN) potential [13] that reproduces fairly well the binding energies of  $A = 2 - 4$  systems. To fine tune the binding energy of  $\alpha$ -particle, the potential strengths of the MN potential are multiplied by 0.9814. The latter contains central and spin-orbit terms whose form factors are specified by symmetrized Woods-Saxon (0.65 and  $1.25 \times 12^{1/3}$  fm for the diffuseness and radius parameters) and its derivative, respectively. The strength parameters of each term,  $V_c^\pi$  and  $V_{ls}^\pi$ , are parity ( $\pi$ ) dependent and set to reproduce the low-lying states of  $^{13}\text{C}$ ,  $-4.95$  ( $1/2^-$ ),  $-1.86$  ( $1/2^+$ ), and  $-1.09$  MeV ( $5/2^+$ ) from  $^{12}\text{C}+n$  threshold:  $V_c^- = -45.78$  MeV,  $V_{ls}^- = 31.08$  MeV fm $^2$ , and  $V_c^+ = -57.57$  MeV,  $V_{ls}^+ = 17.61$  MeV fm $^2$ . The Coulomb potential is included.

To fulfill the Pauli requirement, a solution  $\Psi$  that we want to obtain should satisfy the condition

$$\Gamma_i |\Psi\rangle = 0 \quad (2)$$

for  $i = 1, \dots, 4$ , where  $\Gamma_i$ , acting on the  $i$ th valence nucleon, is a projector to  $0s_{1/2}$  and  $0p_{3/2}$  HO orbits

$$\Gamma = \sum_m |0s_{\frac{1}{2}m}\rangle \langle 0s_{\frac{1}{2}m}| + \sum_m |0p_{\frac{3}{2}m}\rangle \langle 0p_{\frac{3}{2}m}|, \quad (3)$$

where  $m$  runs over all possible magnetic quantum numbers. The radial coordinate of the HO orbit is taken to be the  $CN$  relative distance vector, and the HO frequency  $\hbar\omega$  is set to be 16.0 MeV, which reproduces the size of the  $^{12}\text{C}$  ground state. To practically satisfy the condition (2), we follow an orthogonality projection method [14], in which a pseudo potential  $\lambda \sum_{i=1}^4 \Gamma_i$  with a large value of  $\lambda$  is added to the Hamiltonian and an energy minimization is carried out. By taking  $\lambda = 10^4$  MeV, our solution contains vanishingly small Pauli-forbidden components of the order of  $10^{-4}$ .

The present problem belongs to a class of quantum few-body problems with orthogonally constraints. This type of problem often appears in atomic and subatomic physics when the system contains composite particles [15]. Solving such a problem is quite challenging and much effort has been made to eliminate the forbidden states. Most calculations with the orthogonality constraint have so far been limited to three- or four-body systems. It is only recent that a five-body calculation is performed for  $^{11}_{\Lambda\Lambda}\text{Be}$  in the model of  $\Lambda + \Lambda + \alpha + \alpha + n$  [16], where the pairwise relative motion of  $\alpha - \alpha$  and  $\alpha - n$  contains Pauli-forbidden states. In that hypernuclear case three different relative coordinates are involved in the Pauli constraint, while in our case the Pauli constraint acts on the four  $CN$  coordinates. To our knowledge, we here present a first converged solution for the core plus four-nucleon five-body system.

We find a solution by a variational method. A trial function has to be flexible enough to satisfy several requirements for, e.g., describing different types of struc-

ture and correlated motion of the particles, eliminating the Pauli-forbidden components, and accurately describing the tail of the bound-state wave function in the asymptotic region. The trial function is expressed as a combination of correlated Gaussian (CG) basis states [15, 17, 18],

$$\mathcal{A} \left\{ e^{-\frac{1}{2} \tilde{\mathbf{x}} A \mathbf{x}} [[\mathcal{Y}_{L_1}(\tilde{u}_1 \mathbf{x}) \mathcal{Y}_{L_2}(\tilde{u}_2 \mathbf{x})]_{L\chi L}] \eta_{TM_T} \right\}, \quad (4)$$

with  $\mathcal{Y}_\ell(\mathbf{r}) = r^\ell Y_\ell(\hat{\mathbf{r}})$ . Here  $\mathcal{A}$  is the antisymmetrizer for  $4N$ ,  $\mathbf{x}$  stands for 4 relative coordinates,  $(\mathbf{x}_1, \dots, \mathbf{x}_4)$ ,  $A$  is a  $4 \times 4$  positive-definite, symmetric matrix, and  $u_1$  and  $u_2$  are  $4 \times 1$  matrices (see [18] for detail). The elements of  $A, u_1, u_2$  as well as  $L_1, L_2, L$  are continuous and discrete variational parameters, respectively. The function  $\chi$  ( $\eta$ ) specifies spin (isospin) states of  $4N$ . Possible  $L$  values are 0, 1, and 2. The c.m. motion of the total system is excluded in Eq. (4), and no spurious c.m. motion is included.

The power of the CG basis of type (4) has been demonstrated by many examples [18–20]. An advantage of the CG is that it keeps its functional form under a linear transformation of the coordinates [15, 17], which is a key for describing both cluster and delocalized structure in a unified manner. Each basis element contains so many variational parameters that discretizing them on grids leads to an enormous dimension  $\mathcal{K}$  of at least  $10^{10}$ . Thus we test a number of candidate bases with the stochastic variational method [15, 17, 21, 22], choose the best one among them and increase the basis dimension one by one until a convergence is reached. This procedure costs expensively for computer time but no other viable methods are at hand to get converged solutions for the present problem.

Figure 1 displays the energies of two lowest  $0^+$  states of  $^{16}\text{O}$  versus the basis dimension. More than 9,500 bases are combined to reach the convergence. Most bases, especially up to  $\mathcal{K} = 4,000$ , first serve to eliminate the forbidden states, which is because the use of large  $\lambda$  value to ensure the Pauli principle leads to large positive energies at small basis dimension. The valence nucleons tend to move around the core to gain  $V_{cv}$  and at the same time they want to correlate among them to make use of the attraction of  $V_v$ . Eliminating the forbidden states under such competition is hard. After the ground state energy converges well, the variational parameters are searched to optimize the first excited state at  $\mathcal{K} = 8,000 - 9,000$ . The energy gain after  $\mathcal{K} = 9,500$  is very small. Two  $0^+$  states appear below  $^{12}\text{C} + \alpha$  threshold and their energies are both remarkably close to experiment. Compared to  $^{16}\text{O}$ , the convergence for  $^{16}\text{C}$  is faster: 7,000 bases are enough to describe the weaker correlated motion of  $4N$  and reproduce the ground state energy very well. The obtained energies are listed in Table I. We repeated the calculation with the original MN potential. The binding energy of  $\alpha$ -particle increased by about 1 MeV, but the energies of the two  $0^+$  states from the threshold virtually remained unchanged.

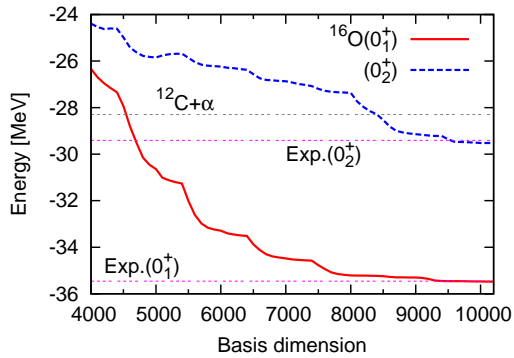


FIG. 1: (Color online) Energies from  $^{12}\text{C}+n+n+p+p$  threshold for the ground and first excited  $0^+$  states of  $^{16}\text{O}$ . The  $^{12}\text{C}+\alpha$  threshold and experimental energies are shown by thin lines.

Analyzing the contribution of each piece of the Hamiltonian to the energy is important to understand the binding mechanism. As listed in Table I, in  $^{16}\text{C}$  the attraction mainly comes from  $V_{cv}$ . In the ground state of  $^{16}\text{O}$ , similarly to  $^{16}\text{C}$ ,  $V_{cv}$  is still a major source of the attraction but  $V_v$  also contributes to the energy significantly, which should not come as a surprise given that the  $np$  interaction is more attractive than the  $nn$  interaction. Since  $\langle V_v \rangle$  is about a half of that of  $\alpha$ -particle, the  $4N$  in the ground state of  $^{16}\text{O}$  are strongly distorted from the intrinsic state of  $\alpha$ -particle due to both the  $CN$  interaction and the Pauli constraint. The first excited state of  $^{16}\text{O}$  exhibits an opposite pattern. The contribution of  $V_v$  is dominating and close to that of  $\alpha$ -particle. It looks that the first excited state has  $^{12}\text{C}+\alpha$  cluster structure as shown by the cluster model [9]. We note, however, that the  $4N$  in the  $0_2^+$  state are not as strongly bound as

TABLE I: Energy contents in MeV and root-mean-square (rms) radii in fm of the  $0^+$  states of  $^{16}\text{O}$  and  $^{16}\text{C}$ . The results of  $\alpha$ -particle are due to a four-body calculation with the MN potential. Empirical rms radii are taken from [23, 24] for  $^{16}\text{C}$  and [25] for  $\alpha$  and  $^{16}\text{O}$ .

|  | $^{16}\text{C} (0_1^+)$ | $^{16}\text{O} (0_1^+)$ | $^{16}\text{O} (0_2^+)$ | $\alpha$ |
|--|-------------------------|-------------------------|-------------------------|----------|
| $E$  | -18.47                  | -35.47                  | -29.52                  | -28.30   |
| $E_{\text{exp.}}$                          | -18.59                  | -35.46                  | -29.41                  | -28.30   |
| $\langle T_{cv} \rangle$                   | 17.81                   | 11.55                   | 7.16                    | -        |
| $\langle V_{cv} \rangle$                   | -82.49                  | -79.55                  | -29.22                  | -        |
| $\langle T_v \rangle$                      | 53.53                   | 72.93                   | 67.46                   | 56.92    |
| $\langle V_v \rangle$                      | -7.32                   | -40.41                  | -74.92                  | -85.22   |
| $\sqrt{\langle r^2 \rangle}$               | 2.62                    | 2.47                    | 3.03                    | 1.43     |
| $\sqrt{\langle r^2 \rangle}_{\text{exp.}}$ | 2.70(3), 2.64(5)        | 2.57(2)                 | -                       | 1.46(1)  |
| $\sqrt{\langle r_{cv}^2 \rangle}$          | 1.94                    | 2.54                    | 4.86                    | -        |
| $\sqrt{\langle r_v^2 \rangle}$             | 2.88                    | 1.90                    | 1.62                    | 1.43     |

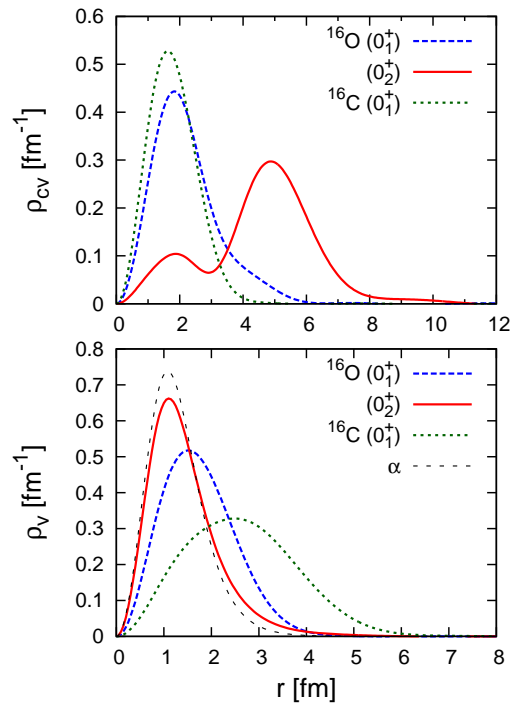


FIG. 2: (Color online). Top: Distributions of the relative distance between the  $^{12}\text{C}$  core and the c.m. of  $4N$ . Bottom: Density distributions of the valence nucleon measured from the  $4N$  c.m. The nucleon density distribution of  $\alpha$ -particle is calculated using the MN potential.

$\alpha$ -particle. In fact the  $4N$  internal energy,  $\langle T_v \rangle + \langle V_v \rangle$ , is only about a quarter of that of  $\alpha$ -particle. The two  $0^+$  states of  $^{16}\text{O}$  have a different face but coexist closely in energy due to the combined function of the  $NN$  and  $CN$  interactions.

The different structure discussed above is visualized by comparing the spatial properties of the three states. Top panel of Fig. 2 shows  $4N$  c.m.-core relative motion distribution,  $\rho_{cv}(r) = \langle \delta(|\mathbf{r}_v - \mathbf{r}_c| - r) \rangle$ , where  $\mathbf{r}_v$  and  $\mathbf{r}_c$  are the coordinates of the  $4N$  c.m. and the core, and bottom one the valence nucleon distribution in  $4N$ ,  $\rho_v(r) = \langle \delta(|\mathbf{r}_1 - \mathbf{r}_v| - r) \rangle$ . In case of  $^{16}\text{C}$ ,  $\rho_{cv}$  is narrow whereas  $\rho_v$  is spread. Four neutrons move on certain orbits with small radii while being apart from each other, indicating an independent particle like motion. In contrast to  $^{16}\text{C}$ , the  $0_2^+$  state of  $^{16}\text{O}$  shows not only extended  $\rho_{cv}$  whose highest peak is at about  $^{12}\text{C}+\alpha$  touching distance ( $\sim 4.9$  fm), but also such narrow  $\rho_v$  that is very similar to the density distribution of  $\alpha$ -particle. This supports that the  $0_2^+$  state of  $^{16}\text{O}$  has  $\alpha$ -cluster-like structure. The distribution of the ground state of  $^{16}\text{O}$  is somewhat intermediate between  $^{16}\text{C}$  and the  $0_2^+$  state of  $^{16}\text{O}$ .

The rms radii are listed in Table I, where, e.g.,  $\langle r_{cv}^2 \rangle$  stands for  $\int_0^\infty r^2 \rho_{cv}(r) dr$ . The point matter radius,  $\sqrt{\langle r^2 \rangle}$ , is obtained assuming the rms radius of  $^{12}\text{C}$  core as 2.33 fm [25]. The matter radii for the ground states of  $^{16}\text{C}$  and  $^{16}\text{O}$  agree with experiment fairly well. Support-

ing the  $\alpha$ -cluster structure,  $\sqrt{\langle r_{cv}^2 \rangle}$  of the  $^{16}\text{O}(0_2^+)$  state is two times larger than that of the  $^{16}\text{O}$  ground state, while  $\sqrt{\langle r_v^2 \rangle}$  is small and slightly larger than the radius of  $\alpha$ -particle. The ratio  $\gamma = \sqrt{\langle r_{cv}^2 \rangle} / \sqrt{\langle r_v^2 \rangle}$  may serve as a measure of clustering. The larger  $\gamma$ , the more prominent the clustering. The  $\gamma$  value is 0.67 for  $^{16}\text{C}$  and grows to 1.3 and 3.0 for the ground and excited states of  $^{16}\text{O}$ . The monopole matrix element,  $|\langle 0_2^+ | r_p^2 | 0_1^+ \rangle|$ , for the two  $0^+$  states of  $^{16}\text{O}$  is  $6.55 \text{ fm}^2$ , somewhat larger than experiment ( $3.55 \pm 0.21 \text{ fm}^2$  [26]), which may be improved by allowing for the excitation of  $^{12}\text{C}$  core.

As a measure of finding  $\alpha$ -particle as a function of the distance  $|\mathbf{r}_v - \mathbf{r}_c|$ , we draw in Fig. 3  $^{12}\text{C}+\alpha$  spectroscopic amplitudes for the two  $0^+$  states,

$$y(r) = \frac{1}{r^2} \langle \phi_\alpha \delta(|\mathbf{r}_v - \mathbf{r}_c| - r) Y_{00}(\widehat{\mathbf{r}_v - \mathbf{r}_c}) | \Psi \rangle, \quad (5)$$

where  $\phi_\alpha$  is the  $\alpha$ -particle wave function obtained with the MN potential. Two curves show a striking difference. In the  $0_1^+$  state, the highest peak is located near the surface region of the core. The spectroscopic factor,  $S_\alpha = \int_0^\infty [ry(r)]^2 dr$ , is small (0.105). Compared to this, the amplitude of the  $0_2^+$  state is much larger and has a peak at  $^{12}\text{C}+\alpha$  touching distance. It is by far larger and longer ranged than that calculated by the deformed model [27]. The  $S_\alpha$  value is 0.680, in agreement with 0.679 of the  $^{12}\text{C}+\alpha$  cluster model [9]. The dimensionless reduced  $\alpha$ -width,  $\theta_\alpha^2$ , at a channel radius  $r$ , defined by  $r^3[y(r)]^2/3$ , is a better measure of  $\alpha$  clustering than  $S_\alpha$ . The value is 0.341 at  $r = 6 \text{ fm}$ , large enough to be compared to that of the negative-parity rotational band based on the  $9.59(1_2^-)$  state of  $^{16}\text{O}$  [9].

The behavior of  $\rho_{cv}(r)$  and  $y(r)$  shown in Figs. 2 and 3 is understood as follows. Letting  $\mathbf{x}_4$  denote  $\mathbf{r}_v - \mathbf{r}_c$ , we may write those functions as

$$y(r) \propto \int d\hat{r} \int d\mathbf{x}_v \phi_\alpha^*(\mathbf{x}_v) \Psi(\mathbf{x}_v, \mathbf{r}), \quad (6)$$

$$\rho_{cv}(r) \propto r^2 \int d\hat{r} \int d\mathbf{x}_v |\Psi(\mathbf{x}_v, \mathbf{r})|^2, \quad (7)$$

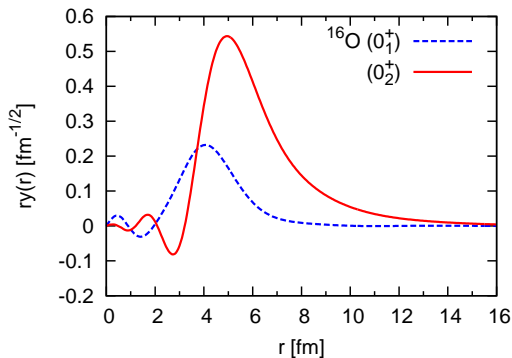


FIG. 3: (Color online).  $^{12}\text{C}+\alpha$  spectroscopic amplitudes for the ground and first excited  $0^+$  states of  $^{16}\text{O}$ .

where  $\mathbf{x}_v$  collectively stands for 3 internal coordinates of the valence nucleons and the spin and isospin coordinates as well as the relevant integration over those coordinates are abbreviated. First we discuss  $y(r)$ . As shown in Fig. 3, the spectroscopic amplitudes for both the ground and first excited states are suppressed and exhibit nodal behavior at short distances. This is because  $\Psi$  contains no  $0s_{1/2}$  and  $0p_{3/2}$  orbits owing to the Pauli principle and  $y(r)$  contains at least  $4\hbar\omega$  HO components. Next we discuss  $\rho_{cv}(r)$ . It is clear from Eq. (7) that  $\rho_{cv}(r)$  is non-negative and its behavior at small  $r$  is determined mainly by those orbits that have relatively small radii such as  $0p_{1/2}, 1s_{1/2}$ , etc. The lower bump of  $\rho_{cv}(r)$  for the excited state is a consequence of the fact that the wave function of the excited state is orthogonal to the ground state wave function.

It is useful to expand the obtained wave functions in terms of the HO basis, especially because the  $0_2^+$  state challenges no-core shell-model description [7]. Explicit expansion is not feasible but counting the number of HO quanta is easy [28]. Figure 4 plots the probability of  $Q\hbar\omega$  components occupied by  $4N$ . The distribution for  $^{16}\text{C}$  and  $^{16}\text{O}(0_1^+)$  is normal: The largest probability occurs at minimum  $Q$  (6 for  $^{16}\text{C}$  and 4 for  $^{16}\text{O}$ ) and decreases rapidly with increasing  $Q$ . The average ( $M_Q$ ) and standard deviation ( $\sigma_Q$ ) of  $Q$ -distribution is 7.0 and 2.1 for  $^{16}\text{C}$ , and 5.5 and 2.9 for the ground state of  $^{16}\text{O}$ , respectively. In contrast with this normal case, the distribution for the excited state of  $^{16}\text{O}$  exhibits a quite different pattern. The probability is widely distributed and not negligible even beyond  $Q = 20$ , with  $M_Q = 14.3$  and  $\sigma_Q = 8.3$ . The peak at  $Q = 10 - 12$  corresponds to  $2 - 4\hbar\omega$  more excitation than  $4p-4h$ . A distribution similar to the  $0_2^+$  case is also obtained for the Hoyle state [28, 29]. Approach like Monte Carlo shell model [30] or no-core shell model with symmetry adaptation [31], importance truncation [32], etc. may be able to describe these states in future but developing an innovative method of calculation will be indispensable.

The core excitation is ignored in the present study. If we allow for the core excitation, we first need to construct the wave functions of both the ground and excited states of  $^{12}\text{C}$  in a microscopic model, and then define the Pauli-forbidden states using those wave functions. In addition, the  $CN$  potential has to be determined consistently with this extended model. According to the  $^{12}\text{C}+\alpha$  cluster model calculation [9], the core excitation can be ignored in the first excited state of  $^{16}\text{O}$  but a certain amount of the excited component is contained in its ground state. This is natural because the core excitation occurs more likely as the valence nucleon gets closer to the core and because the probability of finding the valence nucleon near the core is expected to be much larger in the ground state. If that is the case, in the ground state the energy loss due to the core excitation has to be compensated by some additional attraction of the  $CN$  potential. Thus the consequence of the core excitation will result in shifting the ground state of  $^{16}\text{O}$  towards more delocalized



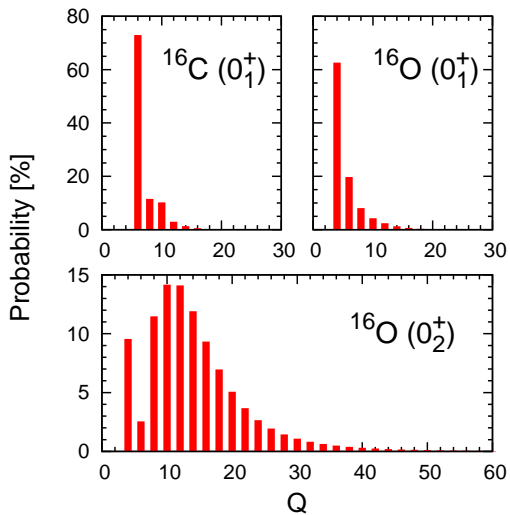


FIG. 4: (Color online). Decomposition of the  $0^+$  states of  $^{16}\text{O}$  and  $^{16}\text{C}$  into  $Q\hbar\omega$  components with  $\hbar\omega = 16.0$  MeV.

structure. Compared to the case with no core excitation, we speculate that the peak position of the spectroscopic amplitude gets closer to the core and the distribution of HO quanta is concentrated more in low oscillator quanta. This possible change of the ground state structure also helps to reduce the monopole strength. Further study along this direction is certainly important for a more detailed description of the shape coexistence in  $^{16}\text{O}$ .

We have attempted to describe simultaneously both the ground and first excited  $0^+$  states of  $^{16}\text{O}$  in the five-body approach of  $^{12}\text{C}$  plus four nucleons. The model

space is large enough to describe the multi-particle multi-hole excitations, the shape coexistence and the  $^{12}\text{C}+\alpha$  clustering. Once the potentials between the particles are chosen to reproduce the energies of the relevant subsystems, neither adjustable parameter nor a bias for the existence of  $\alpha$ -cluster is necessary. The converged solutions for the five-body Schrödinger equation with the Pauli constraint are obtained with the stochastic variational method on the correlated Gaussian basis functions. The ground state of  $^{16}\text{C}$  treated as the system of  $^{12}\text{C}$  plus four neutrons is also examined.

The energies of the ground and first excited states of  $^{16}\text{O}$  as well as the ground state of  $^{16}\text{C}$  are all obtained in very good agreement with experiment. To understand the coexistence mechanism for the two  $0^+$  states of  $^{16}\text{O}$ , we analyze the role of both the core-nucleon and nucleon-nucleon potentials. In the  $0_2^+$  state the four nucleons contribute to gaining energy significantly, suggesting the formation of  $\alpha$ -cluster. The different character of the two states is exhibited by comparing density distributions, particle distances,  $^{12}\text{C}+\alpha$  spectroscopic amplitudes, and probability distributions of harmonic-oscillator quanta. They all exhibit something like a phase transition occurring between delocalized and cluster structure.

As further investigation, it is interesting to include the effect of  $^{12}\text{C}$  core excitation on the spectrum of  $^{16}\text{O}$ . Extending the present approach to heavier nuclei such as  $^{20}\text{Ne}$ ,  $^{40}\text{Ca}$ ,  $^{44,52}\text{Ti}$ , and  $^{212}\text{Po}$  will also be interesting for exploring a possible universal role of  $\alpha$ -like correlation in shape coexistence and  $\alpha$ -decay with an increasing mass number of the core nucleus.

This work was supported in part by JSPS KAKENHI Grant Numbers 21540261, 24540261, and 25800121.

- 
- [1] G. E. Brown and A. M. Green, Nucl. Phys. **75**, 401 (1966).
- [2] D. J. Rowe, G. Thiamova, and J. L. Wood, Phys. Rev. Lett. **97**, 202501 (2006).
- [3] J. L. Wood, K. Heyde, W. Nazarewicz, M. Huyse, and P. Van Duppen, Phys. Rep. **215**, 101 (1992).
- [4] Y. Utsuno and S. Chiba, Phys. Rev. C **83**, 021301(R) (2011).
- [5] M. Bender and P.-H. Heenen, Nucl. Phys. **A 713**, 390 (2003).
- [6] S. Shinohara, H. Ohta, T. Nakatsukasa, and K. Yabana, Phys. Rev. C **74**, 054315 (2006).
- [7] P. Maris, J. P. Vary, and A. M. Shirokov, Phys. Rev. C **79**, 014308 (2009).
- [8] M. Włoch *et al.*, Phys. Rev. Lett. **94**, 212501 (2005).
- [9] Y. Suzuki, Prog. Theor. Phys. **55**, 1751 (1976); *ibid.* **56**, 111 (1976).
- [10] P. Descouvemont, Nucl. Phys. **A 470**, 309 (1987).
- [11] H. Horiuchi and K. Ikeda, Prog. Theor. Phys. **40**, 277 (1968).
- [12] Y. Suzuki, Nucl. Phys. **A 448**, 395 (1986).
- [13] D. R. Thompson, M. LeMere, and Y. C. Tang, Nucl. Phys. **A 286**, 53 (1977).
- [14] V. I. Kukulin and V. N. Pomerantsev, Ann. Phys. (N.Y.) **111**, 30 (1978).
- [15] Y. Suzuki and K. Varga, *Stochastic Variational Approach to Quantum-Mechanical Few-Body Problems*, Lecture Notes in Physics, (Springer, Berlin, 1998), Vol. m54.
- [16] E. Hiyama, M. Kamimura, Y. Yamamoto, and T. Motoba, Phys. Rev. Lett. **104**, 212502 (2010).
- [17] K. Varga and Y. Suzuki, Phys. Rev. C **52**, 2885 (1995).
- [18] Y. Suzuki, W. Horiuchi, M. Orabi, and K. Arai, Few-Body Syst. **42**, 33 (2008).
- [19] W. Horiuchi and Y. Suzuki, Phys. Rev. C **78**, 034305 (2008).
- [20] J. Mitroy *et al.*, Rev. Mod. Phys. **85**, 693 (2013).
- [21] V. I. Kukulin and V. M. Krasnopol'sky, J. Phys. G **3**, 795 (1977).
- [22] K. Varga, Y. Suzuki, and R. G. Lovas, Nucl. Phys. **A 571**, 447 (1994).
- [23] A. Ozawa *et al.*, Nucl. Phys. **A691**, 599 (2001).
- [24] T. Zheng *et al.*, Nucl. Phys. **A 709**, 103 (2002).
- [25] I. Angeli and K. P. Marinova, At. Data Nucl. Data Tables **99**, 69 (2013).
- [26] D. R. Tilley, H. R. Weller, and C. M. Cheves, Nucl. Phys. **A 564**, 1 (1993).

- [27] M. Ichimura, A. Arima, E. C. Halbert, and T. Terasawa, Nucl. Phys. **A 204**, 225 (1973).
- [28] Y. Suzuki, K. Arai, Y. Ogawa, and K. Varga, Phys. Rev. C **54**, 2073 (1996).
- [29] T. Neff, J. Phys. Conference Series **403**, 012028 (2012).
- [30] N. Shimizu *et al.*, Prog. Theor. Exp. Phys. 01A205 (2012).
- [31] T. Dytrych, K. D. Sviratcheva, C. Bahri, J. P. Draayer, and J. P. Vary, Phys. Rev. Lett. **98**, 162503 (2007).
- [32] R. Roth and P. Navrátil, Phys. Rev. Lett. **99**, 092501 (2007).